Research article

Progress in Physical Geography
2026, Vol. 0(0) 1–25

DOI: 10.1177/03091333261422199
journals.sagepub.com/home/ppg
Sage

Holocene peat accumulation rate, hiatus events, and hummock development affected by climate, tephra deposition, and geomorphic setting

Daniel G. Gavin[1], F. Joseph Rocchio[2], John A. Hribljan[3], Katherine A. Heckman[4], Erin M. Herring[1], Jeremy R. Shaw[5] and David J. Cooper[5]

Abstract

Peatland development is affected by changing climates, disturbances such as fire, and autogenic processes. Peatlands may be susceptible to periods of peat loss or reduced accumulation resulting in hiatuses in the peat stratigraphy. At eight minerotrophic peatlands in isolated topographic depressions in western Washington State, peat accumulation rates were reconstructed using radiocarbon-dated continuous peat cores. Age-depth models, fit to 7 to 11 radiocarbon dates and known tephra ages per peatland, were built using a Bayesian approach that constrains the range of potential peat accumulation rates and specifies potential hiatus events at abrupt changes in organic soil composition, tephras, and abrupt changes in the bulk-density profile. The among-site mean long-term rate of organic matter accumulation varied from 30 to 40 g/m^2/year during the Late Holocene but was much lower, 18–22 g/m^2/year, between 9500 and 6500 year before present. Fifteen modeled hiatuses encompassed 22% of the period in the age depths models and were more common during 9500 to 6500 year before present. During this period, hiatuses suggest that 50% of the potential peat accumulation is missing. Compared to nearby pollen and charcoal records, the hiatal intervals were likely the result of peat loss from a lower water table, fire, or burial by 4–7 cm of Mazama tephra. Sites with small watershed:peatland area ratios had the largest hiatuses and small peatlands in kettle depressions had the smallest hiatuses, consistent with water-table sensitivity to climate change. Charcoal and pollen stratigraphy from hummocks at three sites indicate that fires during the last century occurred near the peat core sites with little impact on organic matter accumulation. The variability in peat accumulation, among sites and over time, suggests site-dependent climatic sensitivity of these biologically and hydrologically significant sites.

[1]Department of Geography, University of Oregon, Eugene, OR, USA
[2]Natural Heritage Program, Washington Department of Natural Resources, Olympia, WA, USA
[3]Department of Biology, University of Nebraska Omaha, Omaha, NE, USA
[4]USDA Forest Service Northern Research Station, Houghton, MI, USA
[5]Department of Forest and Rangeland Stewardship, Colorado State University, Fort Collins, CO, USA

Corresponding author:
Daniel G. Gavin, Department of Geography, 1101 Kincaid Street, McKenzie Hall Ste 275, University of Oregon, Eugene OR 97403, Email: dgavin@uoregon.edu

Keywords
age-depth modeling, Pacific Northwest, hiatus, Holocene, peatland, tephra

Introduction

Peatlands are an important part of the landscape habitat mosaic and provide key watershed scale hydrological and ecological functions (Gorham, 1991). However, peatlands that occur near their climatic limit may be susceptible to the changes driven by a warming and drying climate (Charman et al., 2015; Dise 2009). Peat accumulation and preservation depends on the presence of peat-forming plant species and a water table close to the soil surface that limits organic matter decomposition. The water table rises to keep pace with the peat accumulation rate, which is constrained by the climatically and chemically determined limits on primary production and decomposition (Belyea and Baird, 2006; Clymo and Fogg, 1984; Ehnvall et al., 2025). Periods with a water table more than 50 cm below the soil surface may sustain low or negative net ecosystem production (NEP) due to oxidation and/or *in situ* fire, resulting in peat loss and possibly subsidence (Bacon et al., 2017; Belyea and Malmer, 2004). If severe or long-lasting, such events can produce hiatuses in the stratigraphic record of peat accumulation (e.g., Fracasso et al., 2022). Hiatuses may also result from erosion (van Geel et al., 2014). Therefore, peat-accumulation records, constrained by radiocarbon dates, are a valuable record of potentially complex peatland ontogeny.

Syntheses of Holocene peatland development typically reveal regional synchrony of peatland areal expansion (Gorham et al., 2007; Ireland et al., 2013; Liu et al., 2025) and peat accumulation rate histories (e.g., Gorham et al., 2003; Loisel et al., 2014; Zhang et al., 2015). However, few studies in temperate peatlands have systematically modeled and addressed the causes of hiatuses in peatland stratigraphy (Nicholson and Swinehart, 2005; Sim et al., 2023). A study of peat stratigraphy in a forested peatland in the central Congo Basin revealed a Late Holocene hiatus in peat accumulation that occurred during a dry climatic interval (Garcin et al., 2022). Ruwaimana et al. (2024) also found hiatuses related to dry periods in an Indonesian forested peatland. While hiatuses may overprint peat-accumulation records with abrupt temporal gaps, gradual changes in peat accumulation histories may result from continual slow rate of decay in the lower anoxic layers, producing concave age-depth profiles (Clymo and Fogg, 1984).

The goal of this research was to document the accumulation rate across a range of peatlands in the Puget Lowlands in western Washington State, USA (Figure 1) and quantify whether accumulation was consistent over time or whether hiatuses occurred with little to no peat accumulation. As hiatuses originate from processes at the peat surface, we also examined the ages and accumulation profiles of peat hummocks at our sites. To do this, we developed criteria for applying Bayesian age-depth models to identify potential hiatus events. We examined between-site differences to understand a potential role of geomorphic setting on peat accumulation and hiatus occurrence. We develop a regional curve of the "apparent" mean peat accumulation rate that is preserved in the peat stratigraphy, and a regional curve of the estimated missing peat due to hiatus events that would have existed had it accumulated at a constant rate and remained in the profile. We compared these curves with a local pollen record and times of tephra deposition. We hypothesize that peat accumulation was lower, and hiatuses more frequent, during the warmer and drier Early Holocene (11–8 ka, thousands of calibrated years before 1950 CE). At three of our sites, we examined the history of hummock formation via radiocarbon dating, pollen analysis, and charcoal stratigraphy, to address if climate changes and watershed development of the last century has affected peat accumulation.

Study area

The Puget Lobe of the Vashon Glaciation (Figure 1(a)) ablated between 17 and 14 ka, leaving

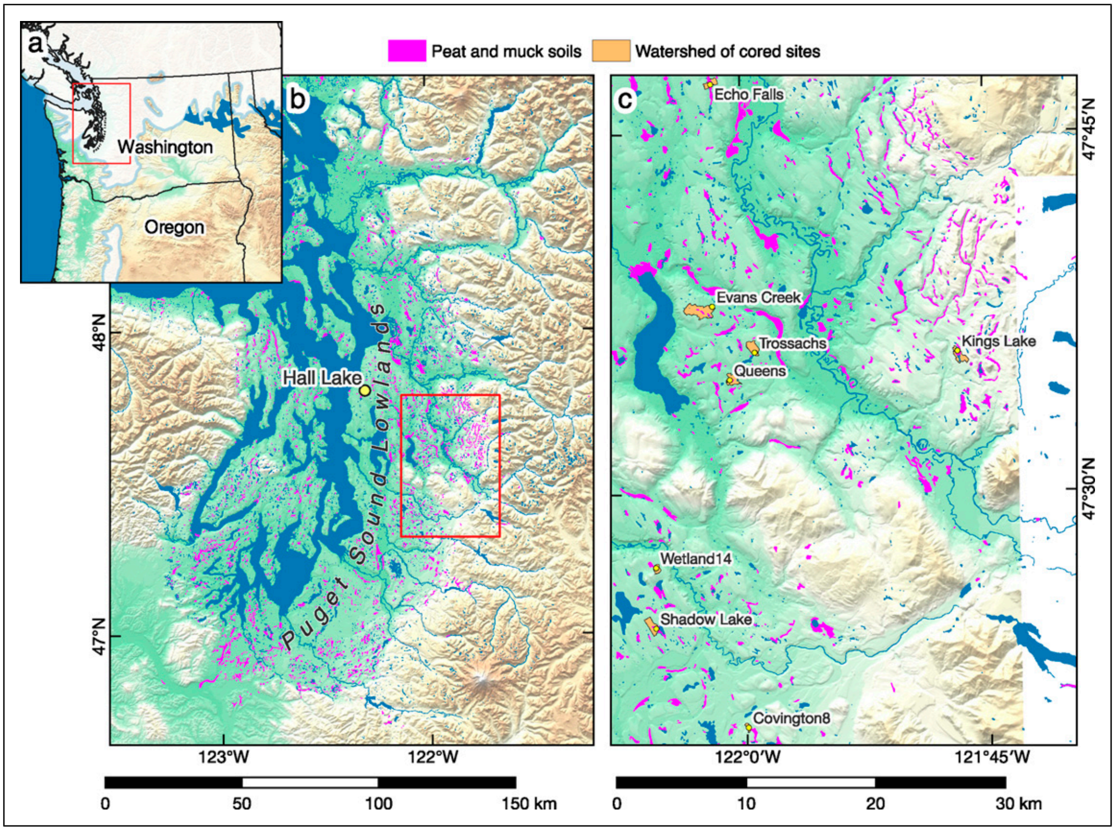

Figure 1. Location of the eight study peatlands in the Puget Lowlands. (a) Overview map showing maximum extent of the Puget Lobe of the Cordilleran Ice Sheet. Red outline shows the extent of map b. (b) Shaded relief of the Puget Lowlands showing, in magenta, the extent of peat and muck soils from the SSURGO soil data base (Soil Survey Staff, 2024). Hall Lake is the site of the comparator pollen record (Sugita and Tsukada, 1982). Red outline shows the extent of map c. (c) Locations of the eight study peatlands. For interpretation of the references to colours in this figure legend, refer to the online version of this article.

behind a compacted sandy to clayey lodgment till with fluted topography, dead-ice terrain with kettle ponds, and outwash channels (Haugerud, 2020; Porter and Swanson, 1998). The compacted sandy to clayey glacial till impedes water flow and supports peatlands and muck soils (Minard and Booth, 1988) in topographic depressions, which comprise 1.9% of the 37,300 km^2 area of the glaciated Puget Basin area lying below 300 m elevation (Soil Survey Staff, 2024; Figure 1). An extensive survey of peatland borings in western Washington in the 1950s revealed that dozens of peatlands contain up to 7 m of peat and mineral sediment, with fibrous peat often overlaying lake sediment (Rigg, 1958). Peatlands in urbanizing regions face stress from changes in hydrological regime and nutrient loading from development, agriculture and atmospheric deposition (Fiałkiewicz-Kozieł et al., 2014; Rocchio et al., 2025).

Sites with no evidence of historical peat mining were selected to represent a range of geomorphic settings (Table 1). Three sites were in fluted glacial scour channels (Covington8, Kings Lake, and Echo Falls). Shadow Lake Bog is also within similar terrain but is affected by the adjacent Shadow Lake. The other four sites (Queens, Evans Creek,

Table 1. Site locations and watershed characteristics of the eight peatlands in this study. See Supplemental Table 1 for vegetation descriptions.

Peatland name	Core location	Elevation (m)	Mean annual precip. (mm) (1991–2020)	Peatland area (ha)	Surrounding surface geology[a]	Inflow exists	Watershed area (ha)	Watershed relief (m)
Covington8	47.33704, −121.99838	206	1420	53.1	Glacial drift, fluted	No	16	24
Queens	47.57869, −122.01336	121	1230	6.6	Ice-contact deposit (kettle depression)	No	63	22
Shadow Lake	47.40665, −122.09174	161	1280	25.8	Glacial till, flute	Yes	74	32
Kings Lake	47.59718, −121.77908	293	1760	39.4	Outwash gravel	No	77	30
Evans Creek	47.62998, −122.03059	117	1180	13.2	Kettle in glacial till	Yes	185	72
Echo Falls	47.78468, −122.02983	125	1260	68.1	Ice-contact deposit, broad hummocky trough	Yes	53	40
Trossachs	47.59765, −121.98751	130	1260	9.6	Kettle in outwash gravel	Yes	72	42
Wetland14	47.44880, −122.09121	156	1220	31.5	Kettle in glacial till	No	29	76

[a]Reported by Washington State Department of Natural Resources

Trossachs, and Wetland14) are in depressions likely formed by dead-ice deposits (i.e., kettle ponds). Many of the peatlands supported hummock-hollow complexes with up to 1 m of relief.

Peatland areas were digitized from lidar topographic data by computing terrain slope and polygonizing the area delimited by abrupt increases in slope. The average slope of the base of the peat was estimated from the depth of the core and the distance from the core site to the nearest edge of the peatland. All sampled peatlands had laggs, transitional zones between the main peat body and adjacent upland or wetland areas (Rocchio et al., 2025).

Many of the peatlands supported hummock-hollow complexes with up to 1 m of relief. Generally, *Sphagnum* spp., fruticose lichens (*Cladonia* spp.), and feathermosses covered the ground surface. *Sphagnum capillifolium* (Ehrh.) Hedw. was the most encountered and generally the most abundant *Sphagnum* species. *Sphagnum fuscum* (Schimp.) Klinggr. and *S. rubellum* Wils. were locally abundant, forming small hummocks or lawns. *Pleurozium schreberi* was common at most sites, and in some locations very abundant. A few sites had very high cover of *Cladonia* spp., *Rhododendron groenlandicum* (Oeder) Kron & Judd and *Kalmia microphylla* (Hook.) A. Heller dominated the shrub

Table 2. Site information regarding peat core length, age, hiatuses, and apparent organic matter accumulation rates (AOMAR). See Supplemental Table 2 for additional parameters for fitting age-depth models.

Peatland name	Core depth (cm)	Uppermost radiocarbon date in core		Number of radiocarbon dates (plus tephra occurrences[b])	Potential hiatus depths (cm)[c]	Mean AOMAR (g/m^2/year)[d]	Mean AOMAR excluding hiatuses (g/m^2/year)[d]	Missing hiatal peat (kg/m^2)[d]
		Depth (cm)	Calibrated date (CE)[a]					
Covington8	319	100	1960	6 (O)	**167, 265**, **281***, **298**	25.4	47.5	104.1
Queens	450[e]	101	1916	8 (O)	133, 369	38.7	39.0	0.3
Shadow Lake	481	103	1895	8 (O)	**185***, **199**, **251**, 361	23.1	29.6	49.4
Kings Lake	507	65	1956	7 (Yn, O)	**176***, **194**, 276, **313***	22.7	48.1	159.0
Evans Creek	606	81	1956	6 (O)	**96***, 361, 513*	28.2	37.6	56.7
Echo Falls	636	94	1955	8 (O, G)	**152, 310**, 583*	29.8	36.1	38.4
Trossachs	698	97	1605	7 (O)	230, 443, **599***	62.0	63.3	3.9
Wetland14	758[e]	103	1440	10 (Yn)	**240**, 368, 568*	59.8	66.1	35.7

[a]Median dates of calibrated radiocarbon ages using the INTCAL20 calibration curve for dates before 1950 CE (Reimer et al., 2020) or the Northern Hemisphere 1 post-bomb calibration curve for dates after 1950 CE (Hua et al., 2022). For all sites except Wetland14, the radiocarbon calibration produced a multi-modal probability density distribution. The age was chosen to be consistent with the pollen profile interpretation or the Bacon age-depth model.
[b]See Supplemental Table 3 for radiocarbon ages. Yn = St. Helens Yn tephra; O = Mazama tephra; G = Glacier Peak tephra.
[c]Hiatuses >50 years identified in the Bacon age-depth models are shown in bold. Potential hiatuses identified subjectively from peat lithology shown by asterisks; others were identified by breakpoints in the bulk-density profile.
[d]Mean apparent organic matter accumulation rate for 0.1 to 6 ka.
[e]Coring did not reach basal sediment.

layer. Tree species were present at all sites, ranging from scattered distribution to nearly closed canopies at a few sites. The abundance of tree species was highest within the shrub layer (0.5 to 5 m height), with *Tsuga heterophylla* (Raf.) Sarg. being the most common species. *Pinus contorta* Doulas ex Loudon var. *contorta*, *Pinus monticola* Douglas ex D. Don, and *Thuja plicata* Donn ex D. Don were occasionally present. Trees taller than 10 m were documented in a few sites and included *Tsuga heterophylla*, *Pinus contorta* var. *contorta*, and *Pinus monticola*. Site-specific vegetation and tree cover is available in Appendix P in Rocchio et al. (2023). Vegetation types of each site were classified using the U.S. National Vegetation Classification (Supplemental Table 1); many of the peatland center and lagg vegetation types are listed as endangered or threatened within Washington State (WADNR, 2025).

Measures of topography, vegetation, hydrology, and pore water chemistry showed that most study sites exhibited chemical indicators of ombrotrophy but evidence of strong downward (recharge) or upward (discharge) movement of groundwater was not apparent at most sites (see Table 2 in Rocchio et al., 2025). Nonetheless, the preponderance of evidence suggests that all sites are predominantly supported by precipitation. Only Evans Creek and Queens Bog showed ombrotrophic characteristics across all measures. Covington8, Echo Falls, Kings Lake, Trossachs, and Wetland14 had conflicting indicators of ombrotrophy. Shadow Lake did not exhibit indicators of ombrotrophic condition.

Methods

Core collection

Cores at each site were obtained at the base of a hummock after sampling the hummock stratigraphy. Due to the soft and loose composition of hummocks, they were sampled by hand. The hummock was sectioned using a shovel and clippers until a clean face was visible. Samples were taken at ca. 10-cm intervals. At three sites (Kings Lake, Evans Creek, and Shadow Lake), a monolith of the hummock was cut from the clean face, wrapped in plastic sheets and used for detailed analysis. Monolith sections spanned the upper 60 to 100 cm of peat. Below the hummock profile, beginning at the uppermost consolidated peat, a continuous core was collected using a 5-cm diameter Russian peat corer (Aquatic Research Instruments, Hope, ID, USA) until corer refusal or until basal non-peat sediments were sampled. Each 50-cm section was photographed in the field, transferred to longitudinally split PVC tubing and wrapped in plastic wrap before transporting to a freezer at Colorado State University. The depths of all samples were referenced relative to the top of the hummock.

Core description, bulk density, and loss-on-ignition

Cores were described by color and texture determined by visual observation and macrofossil composition determined with a microscope. *Sphagnum*, *Pleurozium*, and herbaceous-dominated peats were assigned when macrofossils were observed. Undifferentiated peats (with no clear macrofossil identification) were separated by color (brown, grayish brown, dark gray, and black). Lake sediment (highly organic sapropel; Schnurrenberger et al., 2003) was identified by its fine texture and olive-brown color.

Samples of consolidated peat cores (below the hummock) were analyzed for bulk density (g/cm^3) and organic matter (OM) content (%) via loss-on-ignition (LOI; Chambers et al., 2010). One cm^3 subsamples were obtained at 1 to 13-cm intervals (median 5 cm), for a total of 661 samples. Samples were dried at 80°C until a constant mass, weighed, combusted at 550°C for 4 h, and weighed again.

Ash-free bulk density (OM density; g/cm^3) was calculated as the measured bulk density multiplied by the proportion of organic matter determined by LOI. As total organic carbon (TOC) was not directly measured, we report the percentage of organic matter. Most studies that analyze organic matter and TOC report that TOC is consistently 49 to 53% of OM (Chambers et al., 2010; Loisel et al., 2014). We used the definition of a peatland as containing soils with a C concentration of greater than 12% (24% OM) and a combined peat thickness of at least 40 cm in the upper 80 cm of the peatland (Soil Survey Staff, 2024).

Radiocarbon dating

Depths for 64 radiocarbon dates were chosen to satisfy criteria that dates are spread evenly over the length of each core, with priority for: (1) the top of the consolidated core segments and the core base and (2) four pairs of dates placed approximately 10-cm apart where abrupt changes in peat density (recurrence surfaces) suggest hiatuses, and (3) five dates reserved to examine a 65-cm tall hummock from Kings Lake.

Representative samples of organic matter for radiocarbon dating were chosen from the inside of each core to avoid contamination possibly present on the exterior core surface. All visible roots were removed before analysis. Samples were graphitized in the Houghton Carbon, Water and Soils Laboratory, USDA-Forest Service, Northern Research Station following methods described in Uhelski et al. (2023). Samples from Kings Lake were processed in 2019 and radiocarbon analyses were conducted at the DirectAMS facility, Bothell, WA (Zoppi et al., 2007). All other samples were processed in 2021 and measured at the UCI W. M. Keck Carbon Cycle Accelerator Mass Spectrometry (KCCAMS) Facility at the University of California, Irvine.

Radiocarbon ages were calibrated to the calendar age scale using either the INTCAL20 calibration curve or the Northern Hemisphere zone 1 (NH1) calibration curve for dates with bomb-enriched radiocarbon levels (Hua et al., 2022; Reimer et al., 2004, 2020). An additional 10 tephras with known ages among the eight sites resulted in 7 to 11 age controls per core. The tephras were identified based on their depth relative to radiocarbon dates and mapped areas of tephra deposition (Jensen et al., 2019).

Age-depth modeling and hiatus estimates

It is essential for age-depth models to account for the potential occurrence of hiatuses. We constructed age-depth models using the Bayesian model in Bacon for R statistical software (Blaauw and Christen, 2011). The method simulates peat accumulation by slowly varying the accumulation rate within a range of prior probabilities (i.e., the expected accumulation rate for peatlands) and chooses among millions of simulations those that are the most likely given their fit to the observed radiocarbon dates (Blaauw and Heegaard, 2012). The model does not identify hiatus depths within the model algorithm but rather requires that the depths of potential hiatuses are chosen *a priori*. There is a trade-off in the parameterization of Bacon models. A prior probability of the mean accumulation rate that is slow and non-flexible will constrain the slope of the age-depth relationship requiring longer hiatus events to fit to the radiocarbon dates, while a very flexible prior accumulation rate may adapt to all the radiocarbon dates and not require a hiatus occurrence. Such a flexible prior is reasonable for lake sediments, where sediment accumulation varies due to changing diatom productivity or detrital mineral input and few hiatuses may be expected due to consistently preserved sediment in an often-anoxic environment. However, peatlands accumulate only via net primary productivity at the peatland surface and root zone (Chimner et al., 2002) resulting in a biological limit to the maximum rate of peat accumulation. This justifies a more constrained prior accumulation rate (Goring et al., 2012). The Bacon model does not produce metrics for model selection via parsimony (i.e., contrasting models with hiatuses vs no hiatuses). Therefore, a carefully justified approach is required in the specification of the prior probability distribution of the accumulation rate and the depths of potential hiatuses.

To develop the accumulation-rate prior for our age-depth models, represented by a gamma distribution, we summarized the composite age-depth pattern among our eight sites. The composite age-depth pattern was analyzed on a log-log plot in which a slope of unity corresponds to a constant-accumulation rate. We first subtracted the lower-density and faster-accumulating uppermost peat by referencing depths and ages below the uppermost date (between 65 and 103 cm depth) which was within, or at the top of, the higher-density peat at each site. To assess the variation of the accumulation rate from the composite age-depth scatter plot, we used quantile regression at the 10th, 50th, and 90th percentiles. To develop the accumulation-rate prior distribution for the Bacon model, we chose a gamma distribution informed by these percentile statistics. We confirmed this choice by comparison with peatlands studied by Rigg (1958) who noted the depth of the Mazama tephra aged at 7.633 ka (Egan et al., 2015). From Rigg's report, we used 18 peatlands in King County with continuous sedge, fibrous, or *Sphagnum* peat above the tephra, and the tephra depth at the peatland center to infer the mean accumulation rate. We fit a gamma distribution to these accumulation rates using the fitdistrplus package in R (Delignette-Muller and Dutang, 2015). We also compared our choice to gamma distribution prior developed by Goring et al. (2012) for eastern North American palustrine sites. For lacustrine sediment segments in our cores, we used an accumulation-rate prior that is more flexible and with a higher mean, which is informed by lacustrine sites from Goring et al. (2012) and 12 fen/sedimentary sites from Rigg (1958), using the depth of Mazama tephra. A single exception was the very high accumulation rate of lake sediment at one site (Wetland14). To fit the model to a tephra of known age at this, a very fast accumulation was needed, consistent with fertilization of diatoms by tephra-sourced silica (Baig and Gavin, 2023). Our Bacon models also use a low memory parameter (0.3) and modeling thickness interval (3 cm) to allow the peat accumulation rates to more easily vary within the constraints of the accumulation-rate prior (Supplemental Table 2).

To identify the depth of potential hiatuses, we developed objective criteria based upon organic matter and sediment properties rather than subjective placement of hiatuses to improve the model fit. We expect only a subset of these potential hiatus depths will be utilized in the final fitted models. We used the assumption that past periods of subsidence followed by renewed peat accumulation would result in abrupt changes in the peat bulk density. We used a breakpoint analysis to identify abrupt changes in the ash-free bulk density stratigraphy. We applied the breakpoint function in the strucchange package for R statistical software (Bai and Perron, 2003; Zeileis et al., 2003) with the criteria of at least 10 samples per linear regression segment between breakpoints. The number of breakpoints was determined by a minimum in the Bayesian Information Criterion, a statistic for model selection. Some visually abrupt changes in soil type did not correspond to breakpoints. These changes were often at black layers, which may indicate increased decay because *Pleurozium* macrofossils were observed at the uppermost black layers, or at tephras. These additional potential hiatus depths were added into the Bacon model as well. Increasing the number of radiocarbon dates could more precisely identify hiatuses, but we prioritized extensive sampling of many sites and limited intensive sampling in any one site. Therefore, we acknowledge that some hiatuses in our models, if not bound by radiocarbon dates over short core lengths, may comprise multiple smaller hiatuses or a long period of very slow peat accumulation. The threshold between a hiatus event and low peat accumulation is determined by the lower limit of the accumulation-rate prior probability distribution.

Organic matter accumulation rate

We calculated the down-core profiles of apparent organic matter accumulation rate (AOMAR; g/m^2/year). This "apparent" rate acknowledges that decay may occur throughout the entire depth of the peatland and thus a fraction of mass accumulating at the upper layer of the peatland at the oxic-anoxic interface is lost over millennia, independent of the hiatal events identified in the age-depth model (Clymo and Fogg, 1984; Young et al., 2021). We linearly interpolated bulk density and organic matter between samples to pseudo-annual values. Similarly, we interpolated to pseudo-annual values the accumulation rate from the Bacon accumulation rate estimates at 1-cm intervals. The down-core profile of AOMAR was calculated as the product of the accumulation rate (cm/year), the bulk density (g/cm^3), and the organic matter expressed as a proportion. An estimate of the organic matter represented in hiatuses (i.e., organic matter that could exist if there were no hiatus) was calculated as the mean AOMAR during the 200 year before and after each hiatus. The AOMAR and hiatus estimates were averaged among the eight sites using a robust estimator. We chose the Huber mean to reduce outlier values that have a large effect on our small sample (maximum of 8 sites at any age) yet is more efficient (has a lower variance) than estimators based on the median (Huber and Ronchetti, 2009). The Huber mean requires a tuning parameter to identify extreme values; we used an adaptive tuning method to maximize robustness (Wang et al., 2021). To visualize the effect of uncertainty in the age-depth models on the AOMAR and hiatus estimates, all calculations were repeated for each of the 8000 realizations of the Bayesian age-depth models at each site (Blaauw et al., 2007). Each age-depth model realization had unique accumulation-rate and hiatus start and end dates, resulting in 8000 estimates of the among-site mean AOMAR and hiatus time series, which we summarized as density surfaces. This method only considers uncertainty in the age-depth model and not uncertainty in the proxy measurement (Aquino-López et al., 2024). However, low inter-sample variation in our LOI results, and past studies (Heiri et al., 2001), suggest that the LOI error is likely less than 5%. Other site-level statistics include mean AOMAR (i.e., similar to the long-term rate of carbon accumulation, LORCA; Young et al., 2021), mean AOMAR excluding hiatus periods, and total missing mass in hiatuses (kg/m^2). These were computed for the last-6000-year common period among sites.

Pollen record from Hall Lake

To place the peat accumulation rate history into a paleoclimate and paleovegetation context, we plotted the pollen record from Hall Lake (Sugita and Tsukada, 1982), chosen for its level of detail over the Holocene and proximity to our sites (Figure 1). We digitized pollen percentages for 64 samples from the published pollen diagram and back-calculated the original sample depths using the age-depth model equations from Sugita and Tsukada (1982). We then developed a new Bacon age-depth model from the age basis provided in Sugita and Tsukada (1982): six radiocarbon ages and the depths of the Mazama tephra and the Glacier Peak B/G tephra. We plotted only arboreal pollen percentages, scaled to 100%.

Pollen and charcoal analysis of hummock profiles

Our collected hummock monoliths at three sites were sectioned at 1-cm intervals producing a total of 78 samples for pollen analysis from Evans Creek ($n = 20$), Kings Lake ($n = 23$), and Shadow Lake ($n = 35$). All pollen was extracted from 1 cm^3 peat

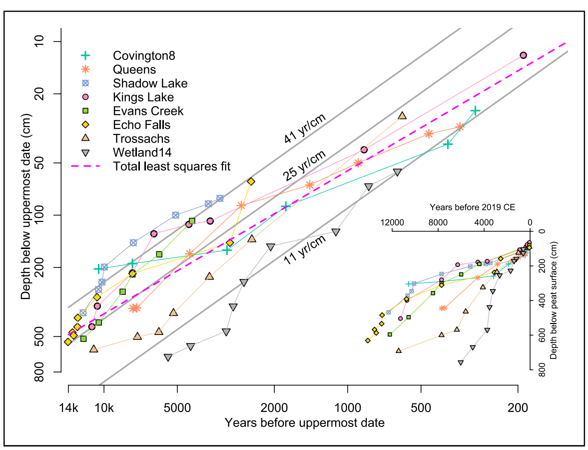

Figure 2. Composite age-depth relationship from median calibrated radiocarbon and tephra ages of eight peat cores. Points are plotted with respect to the uppermost radiocarbon date at each site (Table 2), thus removing the low bulk density peat in the upper ca. 100 cm of each core. The dashed line is a total-least squares regression fit and the isolines show constant peat accumulation rate trajectories at the 10th, 50th, and 90th percentile determined by quantile regression. The inset figure shows the same data plotted on untransformed axes and relative to the peat surface. For interpretation of the references to colours in this figure legend, refer to the online version of this article.

subsamples following standard methods (Fægri and Iversen, 2000). A tablet containing ca. 9666 exotic *Lycopodium* spores was added to each sample for estimating pollen concentration (grains/cm^3). Processed samples were stained with Safranin and pollen was examined at 400X magnification. We identified pollen to the lowest taxonomic level possible based on published keys (Fægri and Iversen, 2000) and the modern pollen reference collection at the University of Oregon. We identified a minimum of 350 terrestrial pollen grains in each sample. For charcoal analysis, continuous 1 cm^3 peat subsamples were extracted from each of the three peat cores ($n = 213$). Charcoal was isolated by wet sieving at two size fractions (>250 μm and 125–250 μm) and particles were tallied under a 40X stereoscope. Charcoal data was expressed as a charcoal concentration (pieces/cm^3).

Age models for three hummock profiles were based on additional radiocarbon dates and the pollen profile. For the Kings Lake hummock, five radiocarbon dates were obtained between 17 and 65 cm and age-depth modeling from 0 to 65 cm was conducted with Bacon software using the post-bomb ("modern") NH1 calibration curve (Hua et al., 2022). For the Shadow Lake and Evans Creek hummocks, too few age-control points were obtained to develop age-depth profiles. Therefore, we used the mean pollen accumulation rate calculated at the well-dated Kings Lake site to assess the other poorly dated sites. Applying the mean pollen accumulation rate (grains/cm^2/year) to the pollen concentration profiles at Evans Creek and Shadow Lake, the age of samples down the profile may be estimated by assuming a constant rate of pollen accumulation (Middeldorp, 1982). The pollen accumulation rate estimate was limited to arboreal pollen excluding *Alnus* to remove the fluctuating contributions of disturbance-related taxa. The age of the base of the hummock profile estimated by pollen concentration was then compared to radiocarbon dates near the bases of the hummocks.

Results

Peat stratigraphy

The eight recovered peat cores ranged from 319 to 758 cm in length (Table 2, Figure 2(a), Supplemental Figure 1). Two cores reached a basal bluish-gray clay, one ended at the Mazama tephra, and one reached a zone with <20% organic matter. All sites consisted of at least 2 m of moss (*Sphagnum* spp. and *Pleurozium* spp.) peat. Five sites (Covington8, Queens, Kings, Shadow, and Evans Creek) consisted entirely of moss peat to their base, while the other three sites began as lakes. Wetland14, Trossachs, Echo Falls, and Wetland14 currently have small areas of open water due to historic peat excavation. Two other sites, Kings and Shadow, are currently lake-margin peatlands that have moss or herbaceous peat to their core base, indicating lower lake levels in the past. Moss peat segments all were marked by organic matter >95% and ash-free bulk density ca. 0.06–0.08 g/cm^3, while lake sediment or herbaceous peat had between 50 and 80% organic matter and more variable bulk density (Figure 3(b)). The breakpoint analysis applied to the bulk-density profiles identified one to three breakpoints per site for a total of 18 breakpoints (Table 2). To identify potential hiatus depths for our age-depth modeling, we selected an additional eight depths among the cores at black layers, tephras, and abrupt changes in organic matter properties.

Age-depth models, organic matter accumulation, and hiatuses

To describe the apparent rate of vertical peat accumulation (cm/year) in the peat profiles, we use the more easily interpreted inverse value, deposition time (year/cm), in which higher values represent lower accumulation rates. After removing the unconsolidated surficial peat and presenting ages and depths below the uppermost radiocarbon date, the composite age-depth scatter plot showed a largely linear age-depth relationship with an average of 25 year/cm and ranging from 11 to 41 year/cm as determined by quantile regression at the 10th and 90th percentiles, respectively (Figure 2). This accumulation rate and its variability was used to set the prior accumulation-rate distribution for age-depth modeling (Supplemental Table 2; Supplemental Figure 2). This accumulation rate is also very similar to that inferred from Mazama depths at

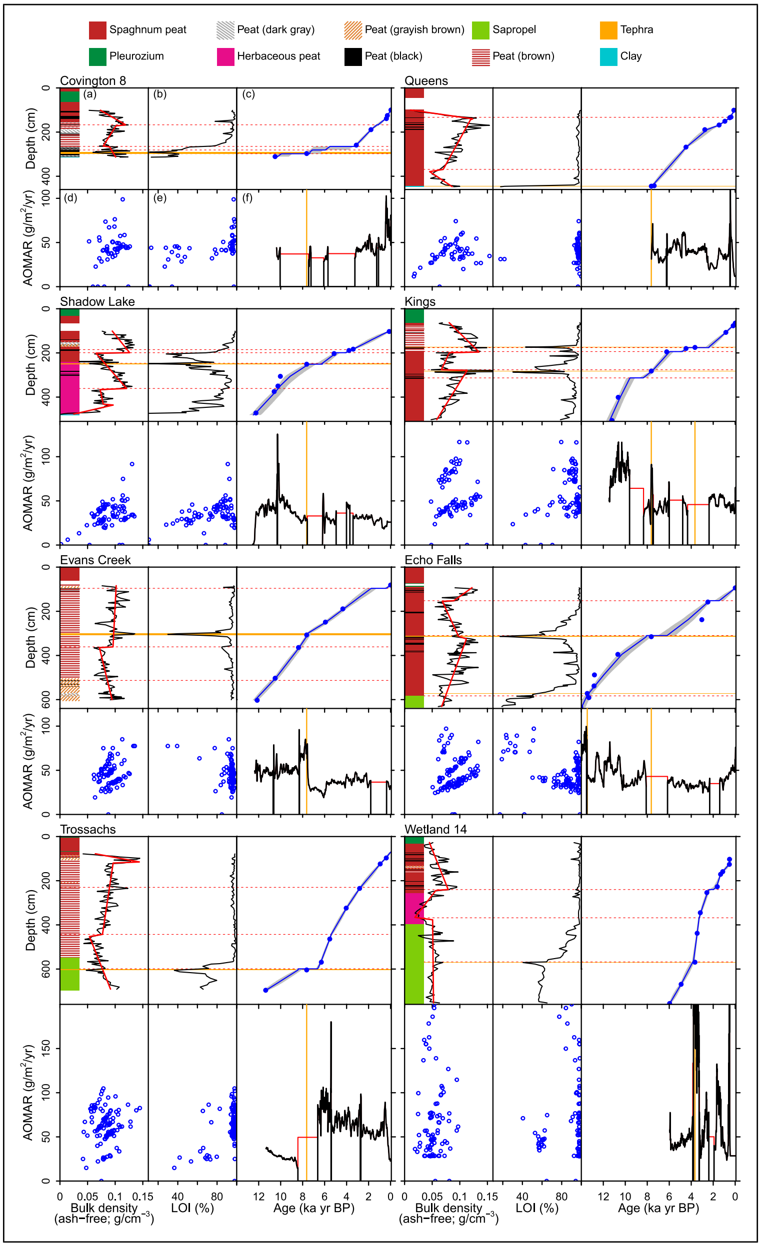

Figure 3. Peat stratigraphy, age-depth model, and apparent organic matter accumulation rate (AOMAR). The top row of each set of six plots per site shows the depth-stratigraphic pattern of (a) peat and sediment types (hatched colors indicate undifferentiated peat types; white areas at Queens, Shadow Lake, and Evans Creek are missing core segments) and ash-free bulk density (OM density; g/cm^3) fitted by the optimal breakpoint model regression (red line), (b) organic matter (%), and (c) the age-depth model showing location of age-control points (blue circles) and the fitted Bacon age-depth model with 95% confidence interval (gray background). Dashed red lines are depths of potential hiatuses in the age model. Orange lines in all plots indicate depths of tephras. The bottom row of each set of plots shows AOMAR in each peat sample plotted with respect to (d) ash-free bulk density, (e) organic matter, and (f) age (years BP). Red lines in plot (f) show the missing peat using mean AOMAR in the 200-year pre-dating and post-dating hiatuses.
For interpretation of the references to colours in this figure legend, refer to the online version of this article.

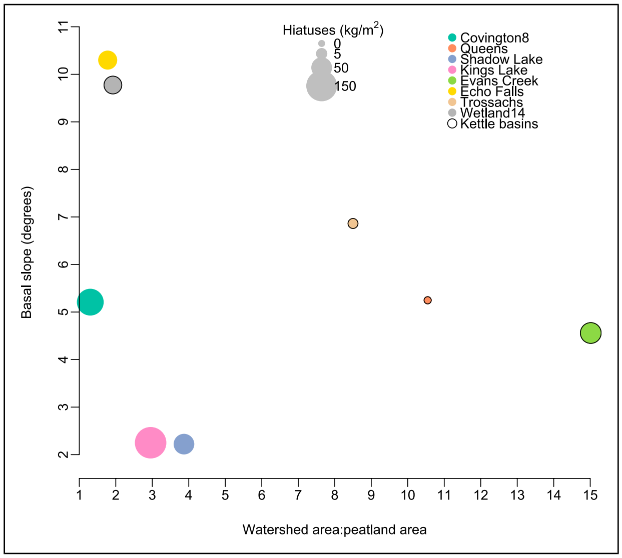

Figure 4. The estimated missing peat in hiatuses in the age-depth models of cores from eight peatlands (as in Figure 3(f)) versus the watershed area:peatland area ratio (Table 1) and the basal slope of the peatland (core depth vs distance to peatland edge). Four kettle-basin peatlands are highlighted with black outline. Hiatal values (Table 2) are for the last 6000-year common period among all cores. For interpretation of the references to colours in this figure legend, refer to the online version of this article.

18 sites in the region (Supplemental Figure 2; Rigg, 1958), and Rigg and Gould's (1957) mean depth of Mazama tephra at 151 peatlands (4.3 m, resulting in 18 year/cm) and the 27 year/cm mean from Goring et al. (2012).

The age-depth relationship in log-log space should have a slope of unity if no changes in accumulation rate occur over time. The curves in Figure 2 visually appear parallel to the constant-accumulation-rate contours except for instances of horizontal segments which are likely related to hiatuses. The total-least squares regression of all eight sites has a slope of 0.82, which indicates a slower accumulation rate (34 year/cm) at 14 ka than at 0.2 ka (15 year/cm). If removing the time span of hiatuses from the age estimates of each radiocarbon age, the best-fit line has a slope of 0.92 resulting in accumulation rates of 22 and 19 cm/year at 14 and 0.2 ka, respectively (Supplemental Figure 3). Therefore, accounting for the 15 major hiatuses results in relatively constant peat accumulation averaged among all sites.

The radiocarbon dates and tephras were in stratigraphic order at all sites (Figure 3). The Bacon age-depth modeling adapted to the radiocarbon dates and tephra ages, resulting in only two radiocarbon dates (at Shadow Lake and Echo Falls) occurring as outliers in the age-depth relationship (Figure 3(b)). Of the 26 potential hiatuses prescribed in the age-depth models, 15 were modeled to be >50 year in length (Table 2). Hiatuses were somewhat more likely in portions of cores with more dense radiocarbon dates: the 15 modeled hiatuses occurred between radiocarbon dates 42 cm apart, on average, while the 11 other core depths that did not result in a modeled hiatus occurred between radiocarbon dates that were 86 cm apart on average. However, this difference was not significant using a Mann Whitney U test ($p > 0.05$). Only nine of the 18 hiatus-depths identified by the breakpoint analysis of the bulk-density profiles resulted in a modeled hiatus, while six of the eight subjectively identified hiatuses resulted in a modeled hiatus (Table 2). Of the four recurrence surfaces visually identified and targeted for radiocarbon dating

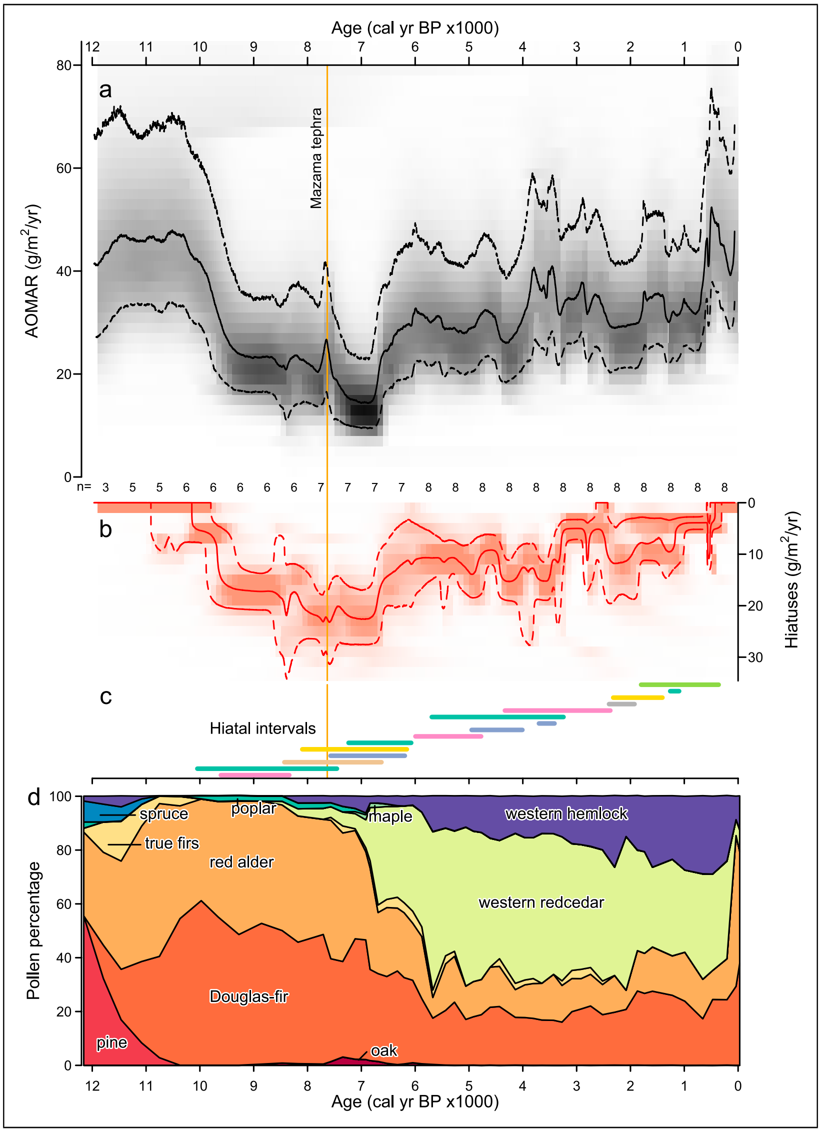

Figure 5. (a) Apparent organic matter accumulation rate (AOMAR) estimated from the robust mean of AOMAR at each site (Figure 3). The number of sites contributing to the mean estimate is shown below the plot. Shaded background shows the probability density of mean estimates from 8000 realizations of the Bayesian age-depth models. Dashed lines correspond to the 10th and 90th percentile of the probability distributions. (b) Estimated missing peat mass in hiatal intervals as shown in Figure 3(f) (red lines), in which hiatuses represent peat that could have accumulated under average conditions. Solid red line is the robust mean among the eight sites. Shaded background as in part (a). (c) The 15 hiatal intervals >50 year in length identified by age-depth modeling, plotted here for the median age-depth model as shown in Figure 3. Colors refer to sites in Figure 2. (d) The pollen record from Hall Lake (Sugita and Tsukada, 1982). Stacked percentages of all arboreal pollen types (summed to 100%) are color-coded and ordered by their relative drought tolerance as reported by Niinemets and Valladares (2006). For interpretation of the references to colours in this figure legend, refer to the online version of this article.

(Supplemental Table 3), two were identified as a modeled hiatus; the other two had similar radiocarbon dates indicating no substantial hiatus event. Full Bacon age-depth model outputs are in Supplemental Figure 4.

Hiatuses occurred throughout the Holocene, and the number and length of hiatuses varied greatly among sites. Two sites with cores that did not reach the Early Holocene (>8.2 ka), Queens and Wetland14, lacked or had only brief hiatuses. Covington8, Shadow Lake, and Trossachs had hiatuses during both the Early and Middle (8.2–4.2 ka) Holocene, and Kings Lake had hiatuses during the Early, Middle, and Late Holocene. Echo Falls had hiatuses during the Middle and Late Holocene, and Evans Creek had a hiatus only during the Late Holocene.

The apparent organic matter accumulation rate (AOMAR) at each site, calculated from the median age-depth model, was generally between 30 and 50 $g/m^2/year$, but punctuated by hiatuses (Figure 3(f)). Mean AOMAR over the last 6000 years varied among sites between 23 and 62 $g/m^2/year$, or 30 to 66 $g/m^2/year$ if the hiatal intervals are excluded from calculations. At sites with widely varying accumulation rates, AOMAR correlated strongly with accumulation rate ($r > 0.7$). In contrast, weak to no correlation exists between AOMAR and bulk density (Figure 3(d); $r = 0.07$ to 0.44 among sites) or AOMAR and organic matter content (Figure 3(e); $r = -0.36$ to 0.54 among sites).

The total missing organic matter in hiatuses, shown as red lines in Figure 3(f), varied greatly among sites (3 to 159 kg/m^2; Table 2). A sample size of eight peatlands is not sufficient for statistical analysis of drivers of these hiatuses. However, because our samples cover a variety of site types, a few patterns emerged (Figure 4). Sites with the greatest hiatus periods, Covington8 and Kings Lake, have small watershed area:peatland area and generally lower basal slope, from core base to peat edge. The four kettle basins, as opposed to peatlands in fluted till or outwash gravel, have less missing peat in hiatuses.

Regional organic matter accumulation and hiatuses

The composite AOMAR record, calculated as the robust (Huber) mean of all sites, shows a distinct minimum between 9.5 and 6.5 ka (18–22 $g/m^2/year$; Figure 5(a)). The early Holocene minimum coincided with a period of longer and more synchronous hiatus events (Figure 5(b) and (c)). During 9.5–6.5 ka, the mean estimated missing peat due to hiatuses (Figure 5(b)) was roughly equivalent to the AOMAR. Uncertainty from the age-depth models, portrayed as the grayscale background in Figure 5(a), shows that low AOMAR was most pronounced in the 1000 year following the Mazama tephra, when four of seven sites have hiatus events (Figure 5(c)). Before 9.5 ka, AOMAR is generally high (>40–45 $g/m^2/year$) though we have fewer sites to contribute to the mean before 10.5 ka. After 7 ka, AOMAR varied from 30 to 40 $g/m^2/year$ with maxima at 4–3 ka and in the last millennium, while the estimated missing hiatal peat was about 5–10 $g/m^2/year$.

The pollen record from Hall Lake (Figure 5(d)) provides a good overall general vegetation history of the Puget Lowland similar to other sites in the region (Cwynar, 1987; Leopold et al., 1982; McLachlan and Brubaker, 1995; Sugita and Tsukada, 1982). Pine pollen (likely shore pine, *Pinus contorta* var. *contorta*), spruce (possibly Sitka spruce, *Picea sitchensis*), and true firs (possibly Pacific silver fir, *Abies amabilis*), decline at the start of the Holocene (11.7 ka) and are replaced by Douglas-fir (*Pseudotsuga menziesii*) and red alder (*Alnus rubra*). Shortly following the Mazama tephra (7.6 ka), mesic shade-tolerant taxa, including western hemlock (*Tsuga heterophylla*) and western redcedar (*Thuja plicata*, represented by Cupressaceae pollen) increase, consistent with a cooler and wetter climate.

Chronology, pollen, and charcoal from peat hummocks

The Kings Lake hummock radiocarbon chronology consisted of five post-bomb radiocarbon dates, the uppermost of which was out of chronological order and not used in the age mode (Supplemental Table 3). The Bacon age model followed the wiggles of the calibrated dates showing an accumulation rate of 0.5 cm/year for the first several decades (before 1990 CE) then increasing to 1.8 cm/year

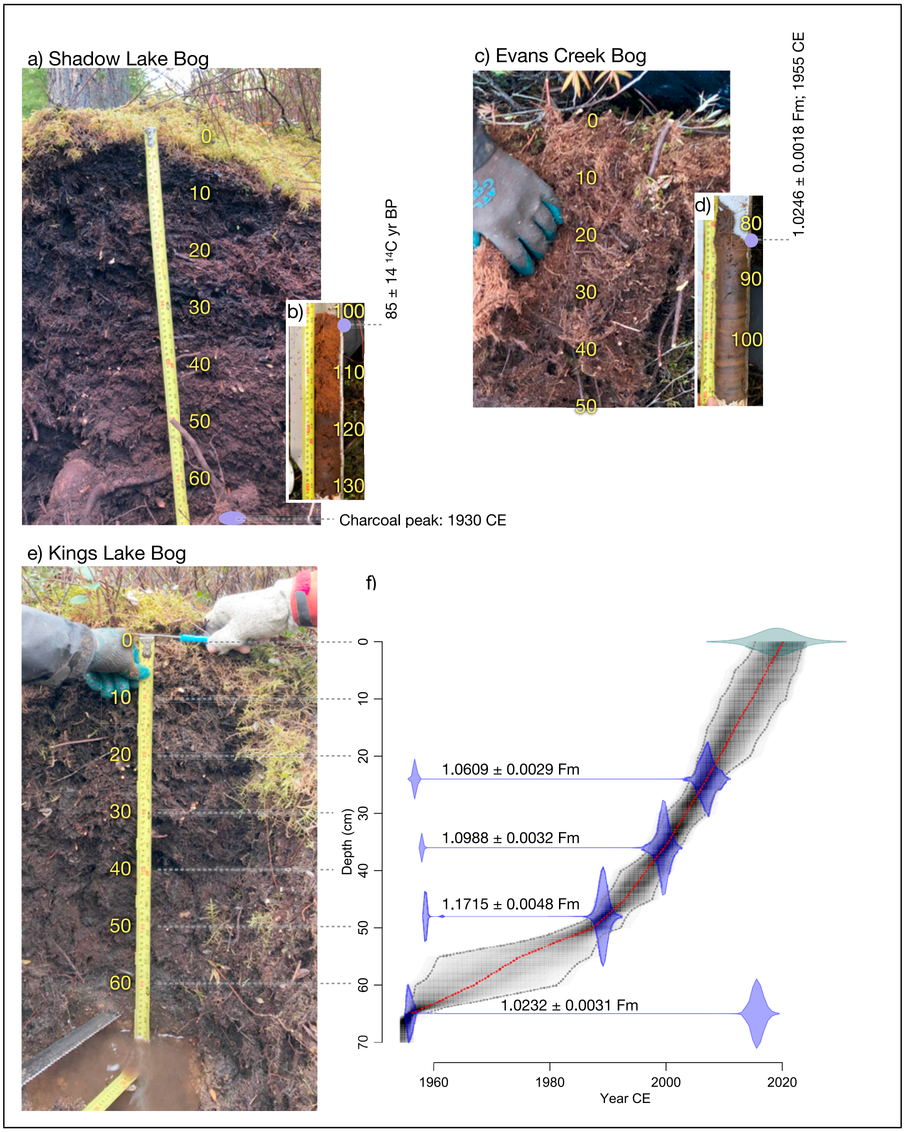

Figure 6. Photos of three hummock cross sections and age-depth diagram of the Kings Lake hummock profile. (a) Shadow Lake Bog hummock cross-section and (b) the uppermost Shadow Lake peat core and radiocarbon date. (c) Evans Creek Bog monolith cross-section and (d) uppermost peat core showing a "modern" radiocarbon date. (e) Kings Lake Bog hummock cross-section, and (f) age-depth model based on four post-bomb radiocarbon ages. Fm = fraction modern radiocarbon. For interpretation of the references to colours in this figure legend, refer to the online version of this article.

over recent decades (Figure 6(f)). The 23 pollen samples from the Kings Lake hummock had an arboreal pollen accumulation rate mean and standard error of 26,100 ± 2700 grains/cm^2/year with no down-profile trend, suggesting it can be used to interpolate ages down-profile (Middeldorp, 1982). Applying this constant pollen accumulation rate to the measured pollen concentrations at Evans Creek resulted in an age at the 53-cm deep hummock base of 1983 CE. A post-bomb radiocarbon date at 81 cm

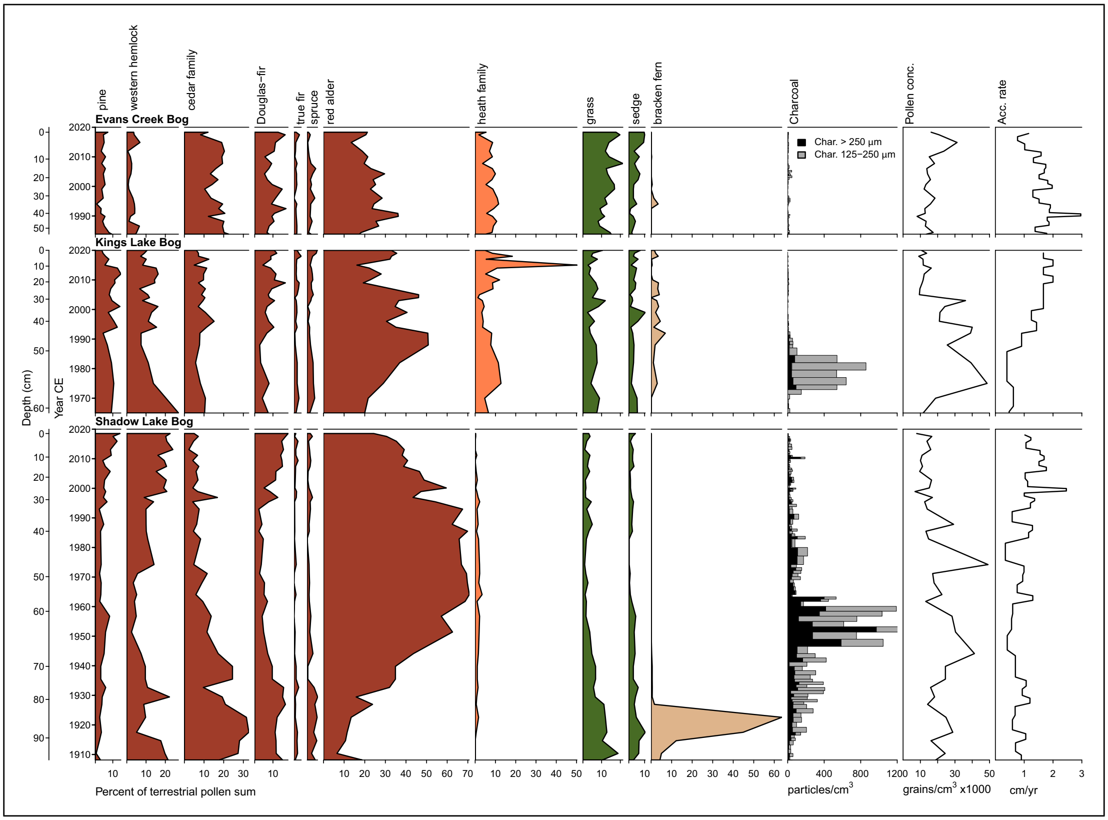

Figure 7. Summary pollen and charcoal diagrams from hummock profiles at Evans Creek, Kings Lake, and Shadow Lake peatlands. Only the most common pollen taxa are shown. Pine pollen represents both lodgepole and western white pine, cedar-family pollen represents western redcedar, true fir represents grand fir, and spruce represents Sitka spruce. Pollen-concentration data shown are arboreal taxa excluding alder. The accumulation rate profile at Kings Lake was determined from the Bacon age-depth model (Figure 6) and at other sites by an assumption of constant arboreal pollen accumulation rate and a radiocarbon age near the base of each hummock. For interpretation of the references to colours in this figure legend, refer to the online version of this article.

calibrates to ca. 1961 CE, consistent with an extrapolation of the pollen-concentration age estimate. At Shadow Lake, a radiocarbon date at 103 cm calibrates to a trimodal probability distribution, the youngest of the three spans is 1873–1915 CE. For the pollen-concentration age estimate of the 97 cm deep hummock base to reach this date, the pollen accumulation rate was adjusted downward to 17,000 grains/cm^2/year. The other five sites lack pollen and charcoal analysis but have uppermost radiocarbon dates consistent with these results. Three sites have uppermost dates near the hummock base suggesting a mean accumulation rate of 1.2 cm/year (Table 1). At Trossachs and Wetland14, older ages at a depth of 1 m (410 and 580 year, respectively) are consistent with these samples being 12 cm or 70 cm below the transition to high density peat.

The pollen and charcoal records reveal disturbances in the landscapes surrounding Shadow Lake and Kings Lake, but not at Evans Creek (Figure 7). The Shadow Lake pollen record begins at 1910 CE with a peak in bracken fern spores (to 60% of the terrestrial pollen sum), followed by a dramatic increase in red alder from 10% to 70%, while conifer trees declined, consistent with regional land clearance. High charcoal concentrations (up to

1200 particles/cm^3) occurred between 1950 and 1970 CE, especially of large fragments >250 µm. The pollen-concentration estimated peat accumulation rate varied from 1 to 2 cm/year. During the last 25 years Douglas-fir pollen increased from 3 to 15% and red alder declined from 70 to 30%. At Kings Lake, a large charcoal peak (800 pieces/cm^3) dated to 1975–1985 CE, also followed by an increase in red alder pollen (20 to 50%). Evans Creek hummock profile encompassed only 35 years and showed little change with depth. Heath-family pollen was common at Evans Creek and Kings Lake (the latter showing a single large peak) but rare at Shadow Lake. Complete pollen diagrams are available in Supplemental Figure 5.

Discussion

The overall peat stratigraphy found at our sites is similar to earlier paleoecological studies in the region (Dachnowski-Stokes, 1930; Hansen and Easterbrook, 1974; Leopold et al., 1982; Rigg, 1958). In contrast to these and many other peatland development studies (e.g., Ratcliffe et al., 2020; Tolonen and Turunen, 1996; Xing et al., 2015), our eight cores and age-depth modeling reveals a previously unrecognized history of hiatus events. Additional radiocarbon dating may revise the hiatus estimates, possibly reducing the length of these hiatuses but also adding more shorter-term hiatuses (Blaauw et al., 2018). Below we address the composite pattern of peatland accumulation rates and potential regional controls of this history (i.e., climate and fire history), and the topographic contexts that may have led to differences in peatland history among the eight sites. We also address recent, within-hummock, organic matter accumulation to assess sensitivity of the peatland to the last century of climate and land-use change.

Holocene climate and tephra effects on peatland history

The apparent carbon accumulation rate, when averaged over 0–6 ka and assuming ca. 50% C content of organic matter, is 18 g C/m^2/year. This is similar to the mean long-term accumulation rates for peatlands on Vancouver Island (Lacourse and Davies, 2015; Lacourse et al., 2019) and in the Colorado Rocky Mountains (Chimner et al., 2002) but roughly half of that reported from temperate peatlands in Europe and China (Charman et al., 2015; Dong et al., 2023; Longman et al., 2021), though there is much variability among temperate peatland sites. Our accumulation rates are also similar to regional accumulation rates of boreal peatlands (Loisel et al., 2014; Yu et al., 2009). Compared to other regional synthesis studies, our long-term regional synthesis shows much greater millennial-scale variability because we explicitly modeled hiatuses. In addition, both the composite age-depth relationship (Supplemental Figure 3) and the trends in AOMAR at each site (Figure 3) are not consistent with the continual slow rate of decay in the lower anoxic layers of the peatland that would produce concave age-depth profiles (Clymo and Fogg, 1984) but are consistent with episodic hiatus events. The lower range of accumulation rates at our sites (41 year/cm) is similar to the distribution from Rigg's (1958) sites (51 year/cm); this end of the distribution differentiated between very slow accumulation and hiatal events.

The 15 hiatuses comprise a significant proportion (22%) of the total time represented in the eight records. Among the eight sites, these hiatuses represent 3 to 160 kg/m^2 of organic matter for the last 6000 years alone that could have accumulated under constant peat accumulation rates. We found mostly asynchronous hiatuses, though there was a cluster of five hiatus end-dates within 1500 years following the Mazama tephra. Overall, the period from 9.5 to 6.5 ka had roughly half the accumulated peat compared to the Late Holocene. Tephra deposition, although only 1–6 cm remaining in the core, may have affected peat accumulation. For example, a study of peat stratigraphy in Japan shows tephra deposition shifted vegetation composition from *Sphagnum* to monocotyledon-dominance (Hughes et al., 2013), and another study from Patagonia showed tephra had transient impact via increased decomposition (Mathijssen et al., 2019). A pollen record for an area near our study sites showed a major Mazama tephra impact on aquatic vegetation

(Egan et al., 2016). Well-drained tephra may limit *Sphagnum* reestablishment, but once it is established, leachates from the tephra may enhance plant growth and peat accumulation (Hughes et al., 2013; Ratcliffe et al., 2020). While five sites had hiatuses following Mazama tephra deposition, at Queens, Kings Lake, and Wetland14 peat accumulation increased for a short time (Figure 3). The deposition and redeposition of ash likely had a heterogeneous influence on our study sites.

Our hiatus estimates do not include the period preceding peat initiation. Radiocarbon dates on macrofossil (wood) samples in the region suggest deglaciation occurred approximately 14.2 ka (Haugerud, 2020). Cores at two of our sites, Shadow Lake and Covington8, had basal blue-gray silty clay, though their basal dates (12.2 and 10.4 ka, respectively) significantly post-date the timing of deglaciation. Three other sites have basal ages between 11.5 and 12.2 ka. The site with the oldest basal date, Echo Falls (14.1 ka; beyond axis limits on Figure 3) is in a light brown silty sediment and is much closer to estimated deglaciation and matches the oldest basal peat age reported by Rigg and Gould (1957). The basal blue-gray sediment indicates that several study basins may have been small lakes or kettle ponds following deglaciation, with wetland vegetation around the edge that eventually filled the lake and formed the peatland. However, this process would have taken thousands of years leading to the relatively young basal peat ages from the middle of the peatlands. In addition, the lack of recessional moraines suggests that the Vashon glaciation ended by ice stagnation (Haugerud, 2020). Buried ice blocks may have persisted for long periods before kettle basins formed and began accumulating peat (Rigg and Gould, 1957). Gorham et al. (2007) synthesized peatland initiation dates across North America and found lags up to 4000 year and suggested dispersal and establishment of ombrotrophic bog taxa, climate change, and the potential role of beavers contribute to the lag.

In addition to tephra impacts, climate during the Holocene imparted trends in organic matter accumulation via the occurrence of longer and more synchronous hiatuses during the Early Holocene. The Early Holocene in western Washington was significantly drier than today due to increased intensity of the Pacific Subtropical High (Kutzbach et al., 1998). Holocene pollen records show a greater relative abundance of drought-tolerant Douglas-fir (*Pseudotsuga menziesii*) and disturbance-adapted red alder (*Alnus rubra*), which increases after fire, and reduction of mesic shade-tolerant taxa, such as western hemlock (*Tsuga heterophylla*) and true firs (*Abies* spp.; Brubaker, 1991; Gavin and Brubaker, 2015). This is illustrated by the major turnover in forest species composition during the Holocene at Hall Lake (Figure 5(d)), with more drought-tolerant taxa dominating during the period of lowest AOMAR and highest hiatus impacts from 9.5 to 6.5 ka. Gallego-Sala et al. (2018) showed that peatlands occur above a threshold moisture index (annual precipitation/annual potential evapotranspiration) of approximately 0.8. Today, the Puget Lowland occurs well above this threshold, with a moisture index of 1.7 (Abatzoglou et al., 2018). However, during the Early Holocene, the moisture index may have been closer to 0.8. A pollen-calibrated precipitation reconstruction for the Early Holocene near our site suggests precipitation was ca. 60% that of today (Brown et al., 2006) and summer insolation was 9% greater during the Early Holocene, which would have increased potential evapotranspiration. Bogs 490 km to the northwest on Vancouver Island also show high carbon accumulation at the start of the Early Holocene, decreasing to a minimum at 7 ka (Lacourse and Davies, 2015), while our sites show an earlier decline in AOMAR. Compared to northern peatland average carbon accumulation history, which peaks from 10 to 7.5 ka (Loisel et al., 2014), the Puget Lowland peatland history is unique but also consistent with regional Holocene hydroclimate and tephra impacts.

Because of the drier climatic conditions, fire was more common during the Early and Middle Holocene (10 to 5 ka) than the Late Holocene in coastal Pacific Northwest forests (Gavin and Brubaker, 2015). In the Puget Lowlands, severe fires led to rapid vegetation change (Crausbay et al., 2017). Future work could develop contiguous macrocharcoal and other geochemical stratigraphies to investigate the role of fire in causing some hiatuses and determine whether the peat surface itself burned

(Zaccone et al., 2014). Peatlands may be fire refugia and burn at low severity if the water table remains near the surface all summer and they do carry fire (Kuntzemann et al., 2023). While some boreal peatlands burn regularly, they are reported to regain their carbon storage function 13 years post-fire (Wieder et al., 2009). The peat accumulation rate had little response to large charcoal peaks at Shadow Lake and Kings Lake (Figure 7). The co-occurrence of a more frequent and severe Early Holocene fire regime and increased hiatuses and reduced peat accumulation may both result from the drier summer climate (Davies et al., 2023; Uhelski et al., 2023).

Topographic controls of peatland history

The eight study sites represent a range of peatland sizes, watershed sizes, and topographic settings, including kettle depressions, flutes in glacial till, and outwash gravels (Table 1, Supplemental Figure 6). Several patterns emerge in the peat accumulation histories and hiatus occurrences with respect to these site characteristics (Figure 4).

Small kettle depressions have few hiatuses. Three kettle sites, Trossachs, Queens, and Evans Creek, are each <15 ha in area with watershed area:peatland area ratios >8 and lack long hiatuses. The one hiatus at Evans Creek is poorly constrained by our radiocarbon dates. A fourth kettle, Wetland14, is a larger peatland, but like Echo Falls which also has low hiatal loss, has a steep basal slope (core base to peatland edge). It appears that sites with stronger hydrological focusing due to a larger relative watershed area and steeper, well-defined basins, are less likely to suffer hiatuses. A study of peat accumulation in Poland also found that peatlands in kettles have the greatest potential for peat accumulation (Karpińska-Kołaczek et al., 2024). These sites may be more likely to maintain stable water tables through droughts. Of the four study kettles, Trossachs and Wetland14 began as lakes and terrestrialized in the Middle to Late Holocene followed by the highest AOMAR of all the sites (>60 g/m^2/year). The surrounding topography may have effectively supported accommodation space as the surrounding water table rose with the accumulating peat body in contrast to a growing peat body rising increasingly higher above surrounding terrain. The Queens core did not reach below the Mazama tephra and lake sediment may occur at greater depths. Evans Creek is the only kettle basin with a full Holocene peat stratigraphy.

Peatlands that formed in fluted till contained the greatest number or length of hiatuses. These sites, Covington8, Kings Lake, and Echo Falls, have elongated shapes reflecting the ice-contact troughs formed by the Vashon Ice Sheet. The Kings Lake area was also affected by glacial outwash. Peatlands in these sites likely formed by primary peat formation on wet mineral soil and spread outward by paludification, as only a brief period of limnic sediment exists at the base of the Echo Falls core. Sustained by small watersheds, the water tables at these sites may be the most responsive to dry periods, leading to peat decomposition. Such sites may also be susceptible to fluvial erosion. Although there is little slope nor gullies on the current peat landforms (Supplemental Figure 6), the role of "bog bursts" (*sensu* van Geel et al., 2014) in causing hiatuses cannot be discounted.

The sites with the lowest AOMAR over the past 6 ka (Shadow Lake and Kings Lake) are adjacent to lakes in which peat accumulation controls the lake outlet. Peat accumulation at these two sites may have raised the lake outlet elevation, as the peat cores reveal *Sphagnum* or herbaceous peat currently at depths well below the current lake level (Supplemental Figure 6). In addition, the longest hiatuses occurred at Kings Lake. These sites may have had fluctuating water levels due to erosion at the lake outlet.

Insights into peat hummock history

Pollen from the low-density hummocks indicate rapid changes in taxon percentages that would not exist if a large proportion of the pollen percolated down the peat profile. Pollen assemblages in the Pacific Northwest, like elsewhere, suffer from overrepresentation of some taxa (e.g., *Alnus and Tsuga*) and underrepresentation of other taxa (*Abies, Pseudotsuga*) relative to their landscape abundance (Gavin et al., 2005). However, the pollen assemblages appear sensitive to the composition of upland vegetation surrounding each peatland and are consistent with secondary succession following logging; the records did not extend to before the logging era.

The partially forested Shadow Lake site experienced peak logging in the 1920s–1940s following construction of the first county roads. This local disturbance is marked by a large peak in bracken fern pollen near the hummock base. The increase in alder represents the opening of the forest canopy on upland areas around the peatland, and grass declined as forested canopy increased. The charcoal peak in the 1950s occurred during the expansion of residential development (Halgren et al., 2011). The high concentration of large charcoal particles suggests a local fire, consistent with charred wood in the area, but we did not detect an impact on peat accumulation. At Kings Lake, located in a region of clearcut plantation forestry, the charcoal peak was in the 1970s and is consistent with clearcut logging near the peatland at that time (Kunze, 1986; Lebednik and del Moral, 1976). The peat accumulation rate at this site, determined by radiocarbon dating, has been increasing since the charcoal peak. Peaks in heath-family pollen, likely Labrador tea that dominates the site today, may simply result from highly local pollen deposition. At Evans Creek higher grass pollen likely represents greater suburban development around the site, otherwise the pollen record shows little change over three decades.

If compaction was progressive down-profile in the hummocks, we would expect to see increasing down-profile pollen concentration and decreasing accumulation rates. Indeed, this pattern was observed at Kings Lake and Shadow Lake, both sites with relatively tall hummocks compared to Evans Creek (Figure 6), though this trend in accumulation rates does not approach accumulation rates during the Holocene, suggesting a more abrupt transition below the analyzed depths. The age-depth relationship at the base of the hummocks (0.8 cm/year) versus in the consolidated peat near the core tops (0.05 cm/year) suggests a sixteen-fold increase in bulk density from the hummock into consolidated peat assuming no additional respirational loss. As sampling bulk density of the heterogeneous hummocks is difficult, we cannot estimate AOMAR within the hummocks to compare to the consolidated peat.

Conclusions

The variety of peat accumulation histories at eight sites in the Puget Lowlands of Washington state agrees with other studies that found high variability in peat accumulation patterns within a single region (Dong et al., 2023; Longman et al., 2021). The long-term rate of organic matter accumulation was similar to nearby Pacific Northwest peatlands but lower than most other lowland temperate peatlands. Hiatuses are likely a major factor in peatland development in topographically constrained sites with small watersheds. The warm and dry period 9.5 to 6.5 ka, clear in the regional vegetation and fire history, resulted in a nearly 50% lower accumulation rate than the Late Holocene. More synchronous hiatuses, possibly also affected by the 7.6 ka Mazama tephra, may explain the lower accumulation rate. However, hiatuses also occurred during the Late Holocene, and we cannot rule out peat erosional events at some sites. Geomorphic setting, as it affects water-table sensitivity to climate, may influence the likelihood of hiatuses. The smallest peatlands in kettle depressions had minimal hiatuses while those with shallow basins and small watersheds had larger hiatuses. Despite the hiatus occurrences, recent peat accumulation in three studied hummocks shows little sensitivity to recent warming or fires of the last century. Additional data from our cores, including testate amoebae, species-level macrofossil identification, and charcoal analysis, would aid in understanding these accumulation-rate histories.

Acknowledgments

We thank Tynan Ramm-Granberg and Monika Ruwaimana for help with field work. We also thank Dr. Mariusz Gałka and four anonymous reviewers for comments on the manuscript.

ORCID iDs

Daniel G. Gavin https://orcid.org/0000-0001-8743-3949

Jeremy R. Shaw https://orcid.org/0000-0003-4338-3454
David J. Cooper https://orcid.org/0000-0003-3391-3538

Ethical considerations

This article does not contain any studies with human or animal participants.

Author contributions

Daniel G. Gavin: Methodology, formal analysis, data curation, writing—original draft, and visualization. F. Joseph Rocchio: Conceptualization, methodology, writing—review and editing, and funding acquisition. John A. Hribljan: funding acquisition, investigation, writing—review and editing. Katherine A. Heckman: investigation, writing—review and editing. Erin M. Herring: investigation. Jeremy R. Shaw: investigation. David J. Cooper: investigation, resources, funding acquisition, and writing—review and editing.

Funding

The authors disclosed receipt of the following financial support for the research, authorship, and/or publication of this article: This project was funded by a Region 10 Wetland Program Development Grant (CD-01J37601) from the U.S. Environmental Protection Agency, a grant from the Colorado Water Center from Colorado State University, and from the Warner College of Natural Resources at Colorado State University.

Declaration of conflicting interests

The authors declared no potential conflicts of interest with respect to the research, authorship, and/or publication of this article.

Data Availability Statement

All raw data are archived on the Neotoma Paleoecology Database (https://neotomadb.org).

Supplemental material

Supplemental material for this article is available online.

References

Abatzoglou JT, Dobrowski SZ, Parks SA, et al. (2018) TerraClimate, a high-resolution global dataset of monthly climate and climatic water balance from 1958–2015. *Scientific Data* 5(1): 170191, Nature Publishing Group.

Aquino-López MA, Anderson L, Sanchez-Cabeza J-A, et al. (2024) Bayesian approaches to proxy uncertainty quantification in paleoecology: a mathematical justification and practical integration. *Journal of Agricultural, Biological and Environmental Statistics*. DOI: 10.1007/s13253-024-00647-5.

Bacon KL, Baird AJ, Blundell A, et al. (2017) Questioning ten common assumptions about peatlands. *Mires and Peat* 19: 1–23.

Bai J and Perron P (2003) Computation and analysis of multiple structural change models. *Journal of Applied Econometrics* 18(1): 1–22.

Baig J and Gavin DG (2023) Postglacial vegetation and fire history with a high-resolution analysis of tephra impacts, high Cascade Range, Oregon, USA. *Quaternary Science Reviews* 303: 107970.

Belyea LR and Baird AJ (2006) Beyond "the limits to peat bog growth": cross-scale feedback in peatland development. *Ecological Monographs* 76(3): 299–322.

Belyea LR and Malmer N (2004) Carbon sequestration in peatland: patterns and mechanisms of response to climate change. *Global Change Biology* 10(7): 1043–1052.

Blaauw M and Christen JA (2011) Flexible paleoclimate age-depth models using an autoregressive gamma process. *Bayesian Analysis* 6(3): 457–474.

Blaauw M and Heegaard E (2012) Estimation of age-depth relationships. In: *Tracking Environmental Change Using Lake Sediments: Data Handling and Numerical Techniques. Developments in Paleoenvironmental Research*. Springer, pp. 379–413.

Blaauw M, Christen JA, Mauquoy D, et al. (2007) Testing the timing of radiocarbon-dated events between proxy archives. *The Holocene* 17(2): 283–288.

Blaauw M, Christen JA, Bennett KD, et al. (2018) Double the dates and go for Bayes — impacts of model choice, dating density and quality on chronologies. *Quaternary Science Reviews* 188: 58–66.

Brown KJ, Fitton RJ, Schoups G, et al. (2006) Holocene precipitation in the coastal temperate rainforest complex of southern British Columbia, Canada. *Quaternary Science Reviews* 25(21–22): 2762–2779.

Brubaker LB (1991) Climate change and the origin of old-growth Douglas-fir forests in the Puget Sound

Lowland. In: Ruggiero LF, Aubry KB, Carey AB, et al. (eds) *Wildlife and Vegetation of Unmanaged Douglas-Fir Forests*. USDA Forest Service, Pacific Northwest Research Station, pp. 17–24.

Chambers FM, Beilman DW and Yu Z (2010) Methods for determining peat humification and for quantifying peat bulk density, organic matter and carbon content for palaeostudies of climate and peatland carbon dynamics. *Mires and Peat* 7(7): 1–10.

Charman DJ, Amesbury MJ, Hinchliffe W, et al. (2015) Drivers of Holocene peatland carbon accumulation across a climate gradient in northeastern North America. *Quaternary Science Reviews* 121: 110–119.

Chimner RA, Cooper DJ and Parton WJ (2002) Modeling carbon accumulation in Rocky Mountain fens. *Wetlands* 22(1): 100–110.

Clymo RS and Fogg GE (1984) The limits to peat bog growth. *Philosophical Transactions of the Royal Society of London. B, Biological Sciences* 303(1117): 605–654, Royal Society.

Crausbay SD, Higuera PE, Sprugel DG, et al. (2017) Fire catalyzed rapid ecological change in lowland coniferous forests of the Pacific Northwest over the past 14,000 years. *Ecology* 98(9): 2356–2369.

Cwynar LC (1987) Fire and forest history of the North Cascade Range. *Ecology* 68: 791–802.

Dachnowski-Stokes AP (1930) Peat profiles in the Puget sound basin of Washington. *Journal of the Washington Academy of Sciences* 20: 193–209.

Davies MA, McLaughlin JW, Packalen MS, et al. (2023) Using Holocene paleo-fire records to estimate carbon stock vulnerabilities in Hudson Bay Lowlands peatlands. *FACETS* 8: 1–26, Canadian Science Publishing.

Delignette-Muller ML and Dutang C (2015) fitdistrplus: an R package for fitting distributions. *Journal of Statistical Software* 64: 1–34.

Dise NB (2009) Peatland response to global change. *Science* 326(5954): 810–811.

Dong Y, Li H, Wang S, et al. (2023) The development process of a temperate montane peatland and its controlling factors since the middle Holocene. *Science China Earth Sciences* 66(3): 594–608.

Egan J, Staff R and Blackford J (2015) A high-precision age estimate of the Holocene Plinian eruption of Mount Mazama, Oregon, USA. *The Holocene* 25(7): 1054–1067.

Egan J, Fletcher WJ, Allott TEH, et al. (2016) The impact and significance of tephra deposition on a Holocene forest environment in the North Cascades, Washington, USA. *Quaternary Science Reviews* 137: 135–155.

Ehnvall B, Ratcliffe JL, Olid C, et al. (2025) Carbon accumulation in recently deposited peat is reduced by increased nutrient supply. *Nature Communications* 16(1): 4271, Nature Publishing Group.

Faegri K and Iversen J (2000) *Textbook of Pollen Analysis*. 4th edition. Blackburn Press.

Fiałkiewicz-Kozieł B, Kołaczek P, Piotrowska N, et al. (2014) High-resolution age-depth model of a peat bog in Poland as an important basis for paleoenvironmental studies. *Radiocarbon* 56(1): 109–125.

Fracasso I, Dinella A, Giammarchi F, et al. (2022) Climate and human impacts inferred from a 1500-year multiproxy record of an alpine peatland in the southeastern alps. *Ecological Indicators* 145: 109737.

Gallego-Sala AV, Charman DJ, Brewer S, et al. (2018) Latitudinal limits to the predicted increase of the peatland carbon sink with warming. *Nature Climate Change* 8: 907–913.

Garcin Y, Schefuß E, Dargie GC, et al. (2022) Hydroclimatic vulnerability of peat carbon in the central Congo Basin. *Nature* 612: 1–6, Nature Publishing Group.

Gavin DG and Brubaker LB (2015) *Late Pleistocene and Holocene Environmental Change on the Olympic Peninsula, Washington*. Ecological Studies 222. Springer International Publishing. DOI: 10.1007/978-3-319-11014-1_1.

Gavin DG, Brubaker LB, McLachlan JS, et al. (2005) Correspondence of pollen assemblages with forest zones across steep environmental gradients, Olympic Peninsula, Washington, USA. *The Holocene* 15(5): 648–662.

Gorham E (1991) Northern peatlands: role in the carbon cycle and probable responses to climatic warming. *Ecological Applications* 1(2): 182–195.

Gorham E, Janssens JA and Glaser PH (2003) Rates of peat accumulation during the postglacial period in 32 sites from Alaska to Newfoundland, with special emphasis on Northern Minnesota. *Canadian Journal of Botany* 81(5): 429–438, NRC Research Press.

Gorham E, Lehman C, Dyke A, et al. (2007) Temporal and spatial aspects of peatland initiation following deglaciation in North America. *Quaternary Science Reviews* 26(3): 300–311.

Goring S, Williams JW, Blois JL, et al. (2012) Deposition times in the northeastern United States during the Holocene: establishing valid priors for Bayesian age models. *Quaternary Science Reviews* 48: 54–60.

Halgren K, O'Connor L and Scott T (2011) *Intensive-Level Survey of Historic Agricultural Resources in King County, Washington*. Washington state department of archaeology and historic preservation. Available at: https://dahp.wa.gov/sites/default/files/HistoricAgriculturalResources_of_KingCounty_2011.pdf (accessed 22 May 2025).

Hansen BCS and Easterbrook DJ (1974) Stratigraphy and palynology of late quaternary sediments in the Puget Lowland, Washington. *Geological Society of America Bulletin* 85: 587–602.

Haugerud RA (2020) Deglaciation of the Puget Lowland, Washington. In: Waitt RB, Thackray GD and Gillespie AR (eds) *Untangling the Quaternary Period—A Legacy of Stephen C. Porter*. Geological Society of America, pp. 279–298.

Heiri O, Lotter AF and Lemcke G (2001) Loss on ignition as a method for estimating organic and carbonate content in sediments: reproducibility and comparability of results. *Journal of Paleolimnology* 25(1): 101–110.

Hua Q, Turnbull JC, Santos GM, et al. (2022) Atmospheric radiocarbon for the period 1950–2019. *Radiocarbon* 64(4): 723–745.

Huber PJ and Ronchetti EM (2009) *Robust Statistics*. John Wiley & Sons.

Hughes PDM, Mallon G, Brown A, et al. (2013) The impact of high tephra loading on late-Holocene carbon accumulation and vegetation succession in peatland communities. *Quaternary Science Reviews* 67: 160–175.

Ireland AW, Booth RK, Hotchkiss SC, et al. (2013) A comparative study of within-basin and regional peatland development: implications for peatland carbon dynamics. *Quaternary Science Reviews* 61: 85–95.

Jensen BJL, Beaudoin AB, Clynne MA, et al. (2019) A re-examination of the three most prominent Holocene tephra deposits in western Canada: Bridge River, Mount St. Helens Yn and Mazama. *Quaternary International* 500: 83–95.

Karpińska-Kołaczek M, Kołaczek P, Marcisz K, et al. (2024) Kettle-hole peatlands as carbon hot spots: unveiling controls of carbon accumulation rates during the last two millennia. *Catena* 237: 107764.

Kuntzemann CE, Whitman E, Stralberg D, et al. (2023) Peatlands promote fire refugia in boreal forests of Northern Alberta, Canada. *Ecosphere* 14(5): e4510.

Kunze LM (1986) Puget trough coastal wetlands: a summary report of biologically significant sites. Phase I: Northern Puget trough impounded Wetlands. Washington Department of Ecology. p. 160.

Kutzbach J, Gallimore R, Harrison S, et al. (1998) Climate and biome simulations for the past 21,000 years. *Quaternary Science Reviews* 17(6–7): 473–506.

Lacourse T and Davies MA (2015) A multi-proxy peat study of Holocene vegetation history, bog development, and carbon accumulation on northern Vancouver Island, Pacific coast of Canada. *The Holocene* 25(7): 1165–1178, SAGE Publications Ltd.

Lacourse T, Beer KW, Craig KB, et al. (2019) Postglacial wetland succession, carbon accumulation, and forest dynamics on the east coast of Vancouver Island, British Columbia, Canada. *Quaternary Research* 92(1): 232–245.

Lebednik GK and del Moral R (1976) Vegetation surrounding Kings Lake Bog, Washington. *Madroño* 23(7): 386–400.

Leopold EB, Nickman R, Hedges JI, et al. (1982) Pollen and lignin records of late-quaternary vegetation, Lake Washington. *Science* 218: 1305–2307.

Liu H, Wu H, Zhang W, et al. (2025) Spatiotemporal distribution of global peatland area during the Holocene. *Scientific Data* 12(1): 37, Nature Publishing Group.

Loisel J, Yu Z, Beilman DW, et al. (2014) A database and synthesis of northern peatland soil properties and Holocene carbon and nitrogen accumulation. *The Holocene* 24(9): 1028–1042.

Longman J, Veres D, Haliuc A, et al. (2021) Carbon accumulation rates of Holocene peatlands in central–eastern Europe document the driving role of human impact over the past 4000 years. *Climate of the Past* 17(6): 2633–2652.

Mathijssen PJH, Gałka M, Borken W, et al. (2019) Plant communities control long term carbon accumulation and biogeochemical gradients in a Patagonian bog. *Science of The Total Environment* 684: 670–681.

McLachlan J and Brubaker LB (1995) Local and regional vegetation change on the northeastern Olympic Peninsula during the Holocene. *Canadian Journal of Botany* 73: 1618–1627.

Middeldorp AA (1982) Pollen concentration as a basis for indirect dating and quantifying net organic and fungal production in a peat bog ecosystem. *Review of Palaeobotany and Palynology* 37(3): 225–282.

Minard JP and Booth DB (1988) Geologic Map of the Redmond Quadrangle, King County, Washington; Map MF-2016. Miscellaneous Field Studies. U.S. Geological Survey.

Nicholson BJ and Swinehart JB (2005) Evidence of Holocene climate change in a Nebraska Sandhills wetland. *Great Plains Research* 15: 45–67.

Niinemets U and Valladares F (2006) Tolerance to shade, drought, and waterlogging of temperate Northern Hemisphere trees and shrubs. *Ecological Monographs* 76(4): 521–547.

Porter SC and Swanson TW (1998) Radiocarbon age constraints on rates of advance and retreat of the Puget lobe of the Cordilleran Ice Sheet during the last glaciation. *Quaternary Research* 50: 205–213.

Ratcliffe JL, Lowe DJ, Schipper LA, et al. (2020) Rapid carbon accumulation in a peatland following Late Holocene tephra deposition, New Zealand. *Quaternary Science Reviews* 246: 106505.

Reimer PJ, Brown TA and Reimer RW (2004) Discussion: reporting and calibration of post-bomb 14C data. *Radiocarbon* 46(3): 1299–1304.

Reimer PJ, Austin WEN, Bard E, et al. (2020) The IntCal20 northern hemisphere radiocarbon age calibration curve (0–55 cal kBP). *Radiocarbon* 62(4): 725–757, Cambridge University Press.

Rigg GB (1958) *Peat resources of Washington*. Bulletin No. 44. Washington Department of Conservation, Division of Mines and Geology. Available at: https://www.dnr.wa.gov/publications/ger_b44_peat_reasources_wa_1.pdf (accessed 13 January 2025).

Rigg GB and Gould HR (1957) Age of the Glacier Peak eruption and chronology of post-glacial peat deposits in Washington and surrounding areas. *American Journal of Science* 255: 341–363.

Rocchio FJ, Ramm-Granberg T, Shaw JR, et al. (2023) *Sphagnum-Dominated Peatlands in the Puget Lowlands: Ecology and Response to Adjacent Land Use*. Natural Heritage Report 2023-01. Washington Natural Heritage Program Washington Department of Natural Resources.

Rocchio FJ, Ramm-Granberg T, Shaw JR, et al. (2025) Hydrogeochemical and vegetation characterization of sphagnum-dominated peatlands in the Puget Lowlands of Washington State, USA. *Wetlands* 45(5): 49.

Ruwaimana M, Gavin DG and Anshari G (2024) Interplay of climate, fires, floods, and anthropogenic impacts on the peat formation and carbon dynamic of coastal and inland tropical peatlands in West Kalimantan, Indonesia. *Ecosystems* 27(3): 361–375.

Schnurrenberger D, Russell J and Kelts K (2003) Classification of lacustrine sediments based on sedimentary components. *Journal of Paleolimnology* 29(2): 141–154.

Sim TG, Swindles GT, Morris PJ, et al. (2023) Regional variability in peatland burning at mid-to high-latitudes during the Holocene. *Quaternary Science Reviews* 305: 108020.

Soil Survey Staff, Natural Resource Conservation Service, United States Department of Agriculture (2024) Soil survey geographic (SSURGO) database for Western Washington. Available online. accessed 15 November 2024.

Sugita S and Tsukada M (1982) The vegetation history in western North America 1. Mineral and Hall Lakes. *Japanese Journal of Ecology* 32(4): 499–516.

Tolonen K and Turunen J (1996) Accumulation rates of carbon in mires in Finland and implications for climate change. *The Holocene* 6(2): 171–178.

Uhelski DM, Kane ES, Heckman KA, et al. (2023) Fire history and long-term carbon accumulation in hemiboreal peatlands. *Ecosystems* 26(7): 1573–1586.

van Geel B, Heijnis H, Charman DJ, et al. (2014) Bog burst in the eastern Netherlands triggered by the 2.8 kyr BP climate event. *The Holocene* 24(11): 1465–1477.

WADNR (2025) *2025 state of Washington natural heritage plan*. Washington Department of Natural Resources.

Wang L, Zheng C, Zhou W, et al. (2021) A new principle for tuning-free Huber regression. *Statistica Sinica* 31: 2153–2177.

Wieder RK, Scott KD, Kamminga K, et al. (2009) Postfire carbon balance in boreal bogs of Alberta, Canada. *Global Change Biology* 15(1): 63–81.

Xing W, Bao K, Gallego-Sala AV, et al. (2015) Climate controls on carbon accumulation in peatlands of Northeast China. *Quaternary Science Reviews* 115: 78–88.

Young DM, Baird AJ, Gallego-Sala AV, et al. (2021) A cautionary tale about using the apparent carbon accumulation rate (aCAR) obtained from peat cores. *Scientific Reports* 11(1): 9547.

Yu Z, Beilman DW and Jones MC (2009) Sensitivity of northern peatland carbon dynamics to Holocene climate change. In: *Carbon Cycling in Northern Peatlands*. American Geophysical Union (AGU), pp. 55–69. DOI: 10.1029/2008GM000822.

Zaccone C, Rein G, D'Orazio V, et al. (2014) Smouldering fire signatures in peat and their implications for palaeoenvironmental reconstructions. *Geochimica et Cosmochimica Acta* 137(Supplement C): 134–146.

Zeileis A, Kleiber C, Krämer W, et al. (2003) Testing and dating of structural changes in practice. *Computational Statistics & Data Analysis* 44: 109–123.

Zhang Z, Xing W, Wang G, et al. (2015) The peatlands developing history in the Sanjiang Plain, NE China and its response to East Asian monsoon variation. *Scientific Reports* 5(1): 11316.

Zoppi U, Crye J, Song Q, et al. (2007) Performance evaluation of the new AMS system at accium biosciences. *Radiocarbon* 49: 173–182.